Manuscript prepared for Clim. Past
with version 3.2 of the LaTeX class copernicus.cls.
Date: 6 October 2011

Supplementary Information for the article: *Heinrich event 1: an example of dynamical ice-sheet reaction to oceanic changes*

Jorge Álvarez-Solas[1,2], Marisa Montoya[1,3], Catherine Ritz[4], Gilles Ramstein[2], Sylvie Charbit[2], Christophe Dumas[2], Kerim Nisancioglu[5], Trond Dokken[5], and Andrey Ganopolski[6]

[1]Dpto. Astrofísica y Ciencias de la Atmósfera, Universidad Complutense, Madrid, Spain
[2]LSCE/IPSL, CEA-CNRS-UVSQ, UMR 1572, CEA Saclay, Gif-sur-Yvette, France
[3]Instituto de Geociencias (UCM-CSIC), Facultad de Ciencias Físicas, Madrid, Spain
[4]Laboratoire de Glaciologie et de Géophysique de l'Environnement, CNRS, Saint Martin d'Hères, France
[5]Bjerknes Centre for Climate Research, Bergen, Norway
[6]Potsdam Institute for Climate Impact Research, Potsdam, Germany

1 The indexation method

In order to obtain the LGM ice-sheet distribution, the GRISLI three-dimensional ice-sheet model of the Northern Hemisphere (Ritz et al., 2001; Peyaud et al., 2007) was forced from 130 ka BP to present using a time-varying climatology (for summer and mean annual surface air temperature as well as mean annual precipitation) for the last glacial cycle. The latter was reconstructed using snapshots from the former CLIMBER-3α LGM climate simulation as well as from a preindustrial climate simulation (Montoya and Levermann, 2008), and an interpolation through time between these snapshots using a glacial index calibrated against the GRIP δ^{18}O record. To minimize errors due to model deficiencies, a perturbative method is used. The time-varying surface air temperature is thus given by:

$$T(t) = T_{CLIM} + (1-\alpha(t)) \times (T_{LGM} - T_{CTRL}), \qquad (1)$$

while precipitation results from:

$$P(t) = P_{CLIM} \times \left[(1-\alpha(t)) \frac{P_{CTRL}}{P_{LGM}} + \alpha(t) \right]^{-1}, \qquad (2)$$

where f_{CLIM} represents the present-day climatology, f_{LGM} and f_{CTRL} are the LGM and control snapshots, respectively, and $\alpha(t)$ is the glacial index. For the present $\alpha = 1$ and the present-day climatology is recovered. The same applies to 130 ka BP. For the LGM $\alpha = 0$ and we recover the present-day climatology corrected by the simulated anomalies. The default treatement of precipitation shown above implies considering high values of the ratio P_{LGM}/P_{CTRL} in areas where the model predicts wet conditions during LGM and arid conditions in the control simulation, especially for $P_{CTRL} \to 0$. In order to avoid this artefact, the term resulting from the perturbative method, f_{per}, has been truncated:

$$f_{per}(t) \equiv \left[(1-\alpha(t)) \frac{P_{CTRL}}{P_{LGM}} + \alpha(t) \right]^{-1} \in [0.0, 2.0] \qquad (3)$$

Additional corrective factors accounting for the surface elevation difference between past and present are also considered. Temperature fields are thus corrected by using a lapse rate index, while the impact of the temperature difference between past and present on the precipitation is accounted for by an exponential term. The procedure is detailed in Charbit et al. (2007) and is based on the assumption that the spatial patterns of temperature and precipitation variations over the last glacial period linearly change with time and, therefore, climatic variations follow the GRIP δ^{18}O record. This approach cannot capture the likely effects of an evolving ice sheet geometry on atmospheric and oceanic circulations. However, this method has been revealed to be very helpful to reconstruct the past Northern ice sheets, especially around the LGM period (Marshall et al., 2000, 2002; Charbit et al., 2002, 2007).

2 Sensitivity experiments

As mentioned in the main text (see sections 2.1 and 2.2), the range of values considered for κ and f ($\equiv \nu^2 \times 10^4$) yields a set of 9 simulations, corresponding to all possible combinations of values of the former parameters. A given configuration of these parameters determines a different configuration of the Northern Hemisphere ice sheets at 18 kBP, prior to Heinrich event 1. The Northern Hemisphere grounded ice volume increases monotonically with increasing drag parameter ν^2, reflecting the fact that ice streams become progressively slower for higher basal dragging coefficients, thus the Laurentide evacuates less ice and its margins become steeper, therefore containing more ice. The basal melting parameter

Correspondence to: J. Alvarez-Solas
(jorge.alvarez.solas@fis.ucm.es)

κ has a certain control on the grounded ice based on the fact that low (high) values facilitate (hinder) a grounding line expansion towards the sea. However, once full glacial conditions are reached (i.e since 60 ka BP), this effect is almost negligible compared to the mentioned effect that different values of ν^2 have on the grounded ice volume. By contrast, the corresponding floating ice volumes decrease by roughly one order of magnitude with increasing κ. Its dependence on ν^2 for a given κ is not monotonic due to the fact that there are two competing processes: Low dragging coefficients (high velocities) favor the occurrence of a fast and relatively shallow ice shelf, while strong friction coefficients imply slower ice streams and thicker ice shelves.

For the lowest range of basal melting parameter κ, a huge ice shelf is simulated in the Labrador Sea. Note that the spatial distribution of ice streams is in very good agreement with other studies based on reconstruction methods (Winsborrow et al., 2004). On the other hand, the very active ice streams flowing from the Hudson Bay/Strait region favor the occurrence of a few partially embayed ice shelves which spatial shape shows a good concordance with that expected by Hulbe et al. (2004). This simulation that has been considered as the standard one in the main text corresponds to $\kappa = 0.5$, $\nu^2 = 2 \times 10^{-4}$. In all cases the results obtained should be considered as underestimating the total ice volume, because the strong AMOC state, with a warmer North Atlantic, was used to scale the GRIP data and/or because in the GRISLI version used herein the presence of sediments is an additional criterium to determine whether a certain area should behave as an ice-stream or not. Under this new criterium, areas potentially treated as ice streams increase resulting in a more reactive ice sheet. This effect is particularly pronounced for the Laurentide where the maximum ice thickness is always below the ICE-5G reconstruction.

3 LIS dynamics dependence on parameter values

We herein show that modest freshwater fluxes that originated from melting of the Fennoscandian ice sheet around 19 ka BP might have induced a reduction of the Atlantic meridional overturning circulation (AMOC) resulting in subsurface warming in the northern north Atlantic and the Labrador Sea, which leads to melting of the Hudson Strait ice shelf and thereby to a Heinrich (H) event. We hypothesize such a mechanism operated during H1.

Recently, deep sea sediment core data from the Nordic Seas have suggested enhanced calving from the Fennoscandian ice-sheet at ca. 19 ka BP leading to enhanced freshwater flux into the Nordic Seas. In order to analyze the possible climatic impacts of such enhanced freshwater flux, an idealized step-function surface freshwater flux perturbation with amplitude varying between A = 0.01-0.5 Sv during a period Δt = 10-100 years was imposed in the northern North Atlantic from 61-63°N and 6°W-5°. This implies, at most, a sea-level rise of up to ca. 1.8 m in as much as 100 years. The latter is consistent with sea-level reconstructions, which show no evidence of a substantial meltwater input at the time (from 15-21 ka BP; cf. Hanebuth et al., 2000; Peltier and Fairbanks, 2006).

Following the freshwater flux perturbation, the surface salinity decreases in the Nordic Seas (not shown), reducing convection in this region. The negative surface salinity anomalies are propagated into the Labrador Sea by the North Atlantic subpolar gyre, thereby contributing to reduce convection as well as deep water formation in the latter region as well.

The responses all basically cluster around two modes: for relatively weak forcing ($\Delta t \leq 20$ year) the AMOC strength is reduced from ca. 22 Sv to ca. 16 Sv and recovers several centuries after the surface freshwater forcing end. For stronger forcing ($\Delta t > 20$ yr), the AMOC is reduced to a value close to that of the stadial state (12 Sv) and does not recover after the freshwater forcing suppression within 2000 years. Each of these two modes shows a different pattern of North Atlantic convection after several centuries, with the less perturbed mode showing a more modest reduction.

The weakened AMOC translates into a reduction of northward heat transport to high northern latitudes, and thereby mean annual SSTs and SATs in the northern North Atlantic and Greenland decrease by up to 4 K.

The 9 Northern Hemisphere ice sheet configurations at 18 ka BP have been equally perturbed by the oceanic subsurface warming resulting from the shift between a strong and a weak AMOC state (Figure 1). As announced above, two main parameters were considered for exploring the phase space of the announced mechanism: the κ-parameter determines the magnitude of basal melting changes as a function of oceanic temperatures, and the ν^2-parameter ($= f \times 10^{-4}$ in the legend of Figure 1) represents a basal friction coefficient in ice streams. As shown in Figure 1, for high values of the κ-parameter a rapid and pronounced first peak of ice discharge is simulated as a response of the ice-shelf collapse. On the other hand, the value of the f-parameter determines the long-term discharge derived from the ice acceleration as a consequence of the former buttressing removal. High values of this latter parameter result in a significant inland ice discharge (if the ice-shelf collapse is efficient enough; excluded for $\kappa = 0.2\ myr^{-1}K^{-1}$). However, high dragging coefficients imply relatively low ice-stream velocities: the loss of thickness near the grounding line is then less pronounced (compared to low values of the f-parameter) and therefore the signal is less efficiently propagated inland, finally explaining the absence of an extended plateau of ice discharge after the first acceleration.

Our results extend those of prevoius works in two ways. First, we have shown that a modest perturbation originated in the Fennoscandian ice sheet, which cannot readily be identified in the sea-level reconstructions, can lead to decrease of deep water formation in the north Atlantic resulting in sub-

surface warming of several degrees. Second, using a state-of-the art ice-sheet model of the Northern Hemisphere including a parameterization of ice shelves we have shown that, within a wide parameter range, the latter subsurface warming can lead to a collapse of the ice-shelf in Hudson Strait and inland ice-streams acceleration possibily explaining H1.

References

Charbit, S., Ritz, C., and Ramstein, G.: Simulations of Northern Hemisphere ice-sheet retreat: sensitivity to physical mechanisms involved during the Last Deglaciation, Quaternary science reviews, 21, 243–265, 2002.

Charbit, S., Ritz, C., Philippon, G., Peyaud, V., and Kageyama, M.: Numerical reconstructions of the Northern Hemisphere ice sheets through the last glacial-interglacial cycle, Clim, Clim. Past, 3, 15–37, 2007.

Hanebuth, T., Stattegger, K., and Grootes, P.: Rapid flooding of the Sunda Shelf: a late-glacial sea-level record, Science, 288, 1033, 2000.

Hulbe, C., MacAyeal, D., Denton, G., Kleman, J., and Lowell, T.: Catastrophic ice shelf breakup as the source of Heinrich event icebergs, Paleoceanography, 19, 2004.

Marshall, S., Tarasov, L., Clarke, G., and Peltier, W.: Glaciological reconstruction of the Laurentide Ice Sheet: physical processes and modelling challenges, Canadian Journal of Earth Sciences, 37, 769–793, 2000.

Marshall, S., James, T., and Clarke, G.: North American ice sheet reconstructions at the Last Glacial Maximum, Quaternary Science Reviews, 21, 175–192, 2002.

Montoya, M. and Levermann, A.: Surface wind-stress threshold for glacial Atlantic overturning, Geophys. Res. Lett., 35, L03 608, doi:10.1029/2007GL032 560, 2008.

Peltier, W. and Fairbanks, R.: Global glacial ice volume and Last Glacial Maximum duration from an extended Barbados sea level record, Quaternary Science Reviews, 25, 3322–3337, 2006.

Peyaud, V., Ritz, C., and Krinner, G.: Modelling the Early Weichselian Eurasian Ice Sheets: role of ice shelves and influence of ice-dammed lakes, Clim, Past, 3, 375–386, 2007.

Ritz, C., Rommelaere, V., and Dumas, C.: Modeling the evolution of Antarctic ice sheet over the last 420,000 years: Implications for altitude changes in the Vostok region, Journal of Geophysical Research-Atmospheres, 106, 31 943–31 964, 2001.

Winsborrow, M., Clark, C., and Stokes, C.: Ice streams of the Laurentide ice sheet, Géographie Physique et Quaternaire, 58, 269, 2004.

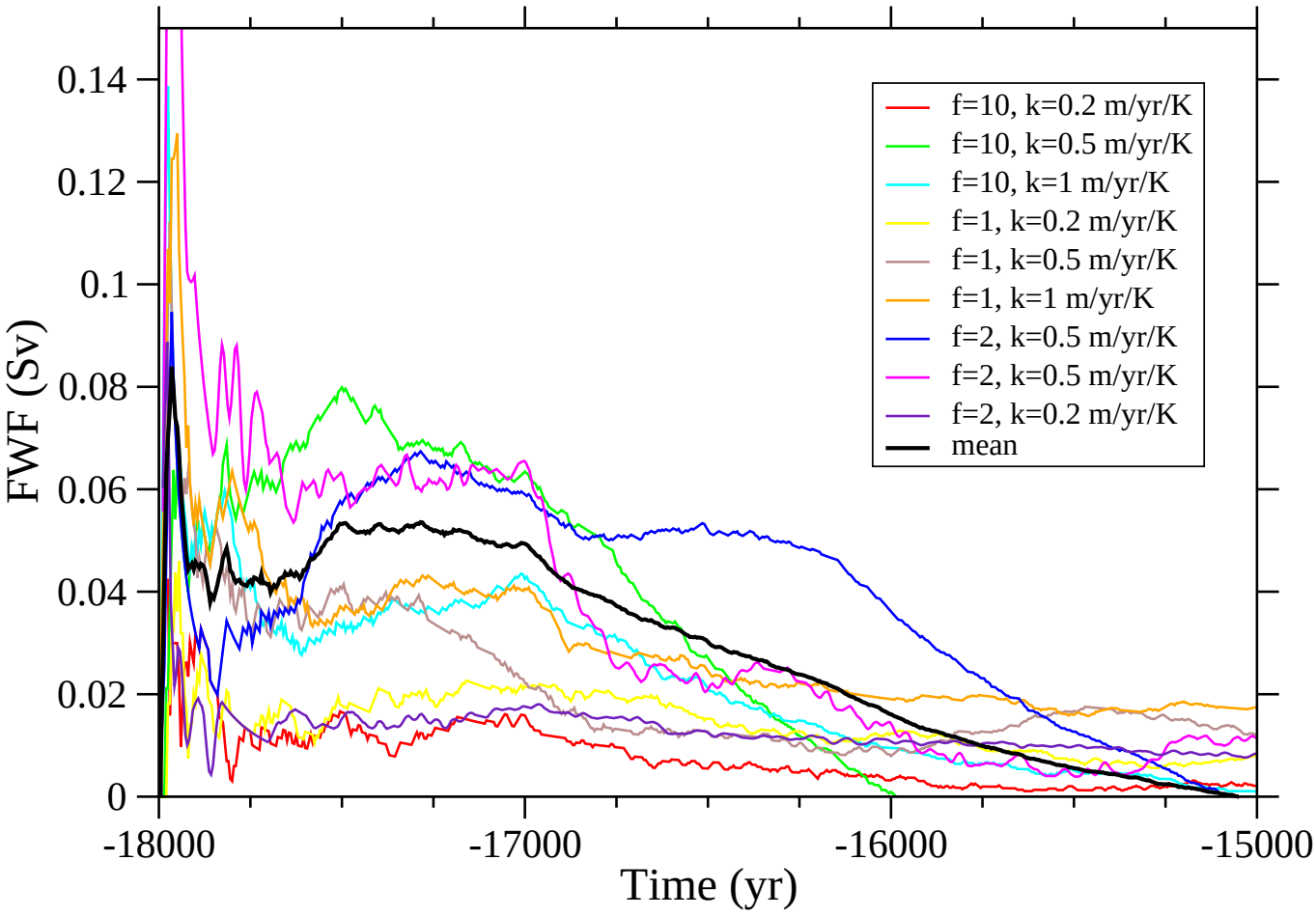

Fig. 1. Iceberg calving (in Sv) derived from the effects of the oceanic subsurface warming on the dynamic behavior of the Laurentide ice sheet for 9 different configurations of the model.